Food and Bioprocess Technology (2021) 14:1700–1711
https://doi.org/10.1007/s11947-021-02669-0

ORIGINAL RESEARCH

Effect of Rice Bran Addition on Physical Properties of Antimicrobial Biocomposite Films Based on Starch

Sofía Berti[1,2] · **Rosa J. Jagus**[1,2] · **Silvia K. Flores**[3,4]

Received: 24 February 2021 / Accepted: 23 May 2021 / Published online: 5 June 2021

Abstract

The increase in consumer requirements for safe and high-quality food has promoted the development of active and edible packaging materials based on biopolymers. In this study, composite tapioca starch films by addition of processed rice bran (PRB) microparticles, containing or not the natural antimicrobials natamycin and nisin, were studied in relation to their physicochemical properties and antimicrobial activity. It was observed that the presence of PRB addition (0.1–0.3% w/w) increased yellowness proportionally to fiber content in films with or without antimicrobials but did not influence on thickness and water vapor permeability. Films with 0.2% PRB allowed the highest increase of tensile strength and strain at break and reduced the solubility in water, showing the optimal compatibility between PRB and starch matrix containing or not antimicrobials. Analysis by FTIR also suggested a good compatibility between filler and matrix through hydrophilic groups. Additionally, the analyzed composite films allowed the diffusion of the natural preservatives verified through zones of inhibition formed in the halo test against *Saccharomyces cerevisiae* and *Listeria innocua*. Consequently, the developed biocomposites can be used as an active packaging for food preservation.

Keywords Rice bran · Starch-based edible film · Physicochemical characterization · Natamycin and nisin · Antimicrobial performance

Introduction

Traditional packaging materials include synthetic polymers derived from petroleum whose residues are not easily assimilated into the environment. This fact, as well as the increase in consumer requirements for safe and high-quality food, has promoted the development of new improved systems, including biodegradable, active, intelligent, and edible packaging. The use of edible, natural, and renewable polysaccharides from plants and animals (cellulose, starch, chitosan, pectins, etc.) in food-packaging applications has emerged as an alternative due to their film-forming properties and environmentally friendly behavior (Daybelis et al., 2015; Gilfillan et al., 2012).

In this context, starch is used to obtain films due to its high availability and great ability to form an odorless, colorless, and transparent polymer matrix (Vásconez et al., 2009) with low oxygen permeability, which is very interesting for food preservation (Jiménez et al., 2012). It is also especially attractive because of its biodegradability and low cost (Lafargue et al., 2007).

Nevertheless, starch films present some drawbacks: unstable mechanical properties due to the retrogradation phenomenon and a relatively high water vapor permeability (Wan et al., 2015). Plasticizers are usually added to improve processing by softening the polymer so that it can be ductile at room temperatures (Avérous & Halley, 2009). Additionally, starch is hygroscopic because hydroxyl groups presence.

Rosa J. Jagus and Silvia K. Flores contributed equally to the manuscript.

✉ Sofía Berti
bsofia@fi.uba.ar

1 Departamento de Ingeniería Química, Facultad de Ingeniería, Universidad de Buenos Aires, Intendente Güiraldes 2620, 1428 Ciudad Autonoma de Buenos Aires, Argentina

2 Instituto de Tecnologías y Ciencias de la Ingeniería (INTECIN), CONICET - Universidad de Buenos Aires, Buenos Aires, Argentina

3 Departamento de Industrias, Facultad de Ciencias Exactas y Naturales, Universidad de Buenos Aires, Intendente Güiraldes 2620, 1428 Ciudad Autonoma de Buenos Aires, Argentina

4 Instituto de Tecnología de Alimentos y Procesos Químicos (ITAPROQ), CONICET - Universidad de Buenos Aires, Buenos Aires, Argentina

However, this nature can be counteracted by adding natural fillers like cellulose microfibers or nanofibers, which have been shown to improve water resistance, tensile strength, and Young's modulus (Cerqueira et al., 2009).

In order to improve the barrier and mechanical properties of starch films, different authors formulated starch-based matrix with protein such as zein (Pérez et al., 2021) or nanopacked Jamaica flower extract (Toro-Márquez et al., 2018) or with natural fibers from vegetable. In this sense, Chen et al. (2009) reported that film transparency, tensile strength, elongation at break, and water barrier properties were improved when pea shell fiber nanoparticles were incorporated in pea starch films. In addition, other authors also formulated composite films, incorporating natural fibers such as passion fruit peel (Moro et al., 2017), kenaf (Zainuddin et al., 2013), luffa (Kaewtatip & Thongmee, 2012), and jute (Prachayawarakorn et al., 2013). Similarly, Ollé Resa et al. (2021) analyzed edible tapioca starch films reinforced with pumpkin bran and oatmeal fillings. Such biocomposites develop strong bonds between the fiber and the starch matrix improving mechanical properties. When the fibers have a good dispersion in the matrix, avoiding agglomeration, optimal resistance is achieved (Gilfillan et al., 2012).

A novel and interesting natural fiber source can be found in rice bran, one of by-products of commercial rice after the milling process. It is known that rice bran represents about 10% of the grain weight and contains good-quality biological proteins, fats, and starch. Depending on the variety of rice and the type of processing, rice bran contains about 15–20% fat, 12–16% protein, 23–28% fiber, and 7–10% ash. In order to take advantage of this by-product, different applications have been proposed that include addition of filler in biopolymer-based films, being of great interest at present. Cano et al. (2014) evaluated the effect of the amylose:amylopectin ratio and rice bran addition on mechanical properties of starch films. They observed more resistance to fracture and less extensible films and an improvement of the elastic modulus when rice bran with lower particle size (<57 μm) was used.

A relevant functionality of active packaging films is their ability to modulate the content of additives (antioxidants, antimicrobials, etc.) in food interfaces or surfaces (Basch et al., 2013). They allow additives to release slowly, increasing their action for a longer time, and maintaining their concentration on the surface. In turn, it contributes to the protection of these additives by reducing interactions with the components of the food matrix. In particular, nisin, an antibacterial peptide produced by strains of *Lactococcus lactis* subspecies *Lactis*, showed antimicrobial activity towards a wide range of gram-positive bacteria, including *L. monocytogenes* and is considered GRAS (Generally Recognize As Safe). In this respect, Ge et al. (2017) demonstrated an antimicrobial activity against *Staphylococcus aureus* owning to the addition of nisin in biodegradable gelatin-based edible films reinforced with amino-functionalized montmorillonite. Likewise, natamycin, an antifungal produced by *Streptomyces natalensis*, showed activity against molds in several foods and has been approved as a food additive in more than 40 countries. Costa et al. (2018) mentioned that the incorporation of antimicrobials as natamycin in the starch-based coating resulted in a reduction of the yeast and mold spoilage. Recently, Berti et al. (2020) demonstrated that the starch-based films added with rice bran and containing natamycin and nisin reduced the surface contamination of *Listeria innocua* and *Saccharomyces cerevisiae*, improving the microbiological quality of Argentinian Port Salut cheese.

To the best of our knowledge, the present research proposes for the first time the combined use of a natural by-product from rice industrialization and natamycin and nisin as natural antimicrobial to produce a biocomposite and active packaging material based on starch with the aim to find a formulation that optimizes its physical properties and, at the same time, maintains an effective protective action against spoilage microorganisms to guarantee a safe product.

The objective of the present work was to study the effect of rice bran addition on the physical properties of biocomposite edible films based on tapioca starch and added or not with natamycin (antifungal) and nisin (antibacterial). Moreover, the diffusion of antimicrobials incorporated into films to a model system was evaluated.

Materials and Methods

Materials

Tapioca starch was provided by Bernesa S.A. (Argentina) and glycerol by Mallinckrodt (Argentina). Commercial natamycin (Delvocid® Salt) and commercial nisin (Nisin®) were provided by DSM (The Netherlands). Rice (*Oryza sativa*) bran was provided by Cooperativa Arroceros Villa Elisa (Entre Ríos, Argentina). Chemicals were of analytical grade.

Rice Bran Processing

Crude rice bran was processed according Berti et al. (2020) in order to obtain a safe product categorized by size. Briefly, a rice bran aqueous suspension (1:10) was sterilized, cooled, and washed twice with distilled water. Then, solids were separated by centrifugation and freeze-dried. The powder was ground and classified by sieves. The processed rice bran (PRB) with a size smaller than 105 μm was characterized.

Physicochemical Characterization of Processed Rice Bran

The proximate analysis of PRB was determined as follow and the results were expressed as g/100 g sample:

- Moisture. Samples were dried in a vacuum oven at 100 ºC for 24 h (AOAC 934.01, 2005).
- Ashes. Calcination was carried out at 500 ºC in a muffle (O.R., Apollo, Argentina) (AOAC 942.05, 2005).
- Protein. Samples were treated by Lowry method (Lowry et al., 1951).
- Fiber. The neutral detergent method (AOAC 991.42, 1998) was applied to determine the insoluble dietary fiber content.
- Lipids: Samples were extracted with petroleum ether in a Soxhlet device (AOAC 960.39, 2005).
- Carbohydrates: it was calculated by subtracting the percent values of other components from 100.

The particle size distribution of processed rice bran

Was determined at room temperature by static light scattering using a Mastersizer 2000 (Malvern Instruments, England) provided with a He–Ne laser (λ 633 nm). The size distribution was described using the diameters (μm) d(0.1), d(0.5), and d(0.9). These values indicate that 10%, 50%, and 90% of the cumulative population corresponds to particles with a diameter smaller than d(0.1), d(0.5), and d(0.9) respectively; the D[3,2] surface–weighted mean diameter (Sauter diameter, μm); and the D[4,3] volume–weighted mean diameter (De Brouckere diameter, μm).

Scanning electron microscopy

Was performed to observe the PRB morphology, using a Zeiss Supra 40 (Carl Zeiss, Germany) microscope. Briefly, samples were dried on $CaCl_2$ and then mounted on a bronze stub and sputter coated (Cressington Scientific Instruments Sputter Coater, UK) with a layer of gold prior to imaging (Alzate et al., 2017).

Film Preparation

Different mixtures of film-forming solutions were prepared according to Table 1. Slurries were heated, and starch gelatinization was performed at ~1.5 °C min^{-1} till 82–85 °C (Ollé Resa et al., 2014). Briefly, water was stirred with glycerol in a beaker; after 10 min, the starch and PRB were added and stirring was continued with controlled heating. The natamycin and nisin (NANI) solution was added to antimicrobial films when the temperature was ~65 °C. The film-forming solutions were dispensed in silicon plates (15 g) and dried during 20 h at 40 °C. Finally, the constituted films were conditioned at 25 °C and 57% relative humidity before carrying out the different tests.

Table 1 Composition of different films based on tapioca starch

Film	Starch	Glycerol	Processed rice bran	Nisin	Natamycin
C	5	2	--	--	--
S1	5	2	0.1	--	--
S2	5	2	0.2	--	--
S3	5	2	0.3	--	--
CNANI	5	2	--	0.027	0.0068
SNANI1	5	2	0.1	0.027	0.0068
SNANI2	5	2	0.2	0.027	0.0068
SNANI3	5	2	0.3	0.027	0.0068

Values expressed as g 100 g^{-1} slurry. In all film formulations, 100 g of slurry was completed with distillated water

Physicochemical Characterization of Films

- Color evaluation was carried out using a Minolta colorimeter (Minolta CM-508d, Japan). The CieLab parameters, L*, a*, and b* and yellowness index (YI) were measured in at least five positions randomly selected. The YI was calculated according to ASTM D1925 (1988) following Eq. (1):

$$YI = \frac{100}{Y}(1{,}2769\ X - 1{,}0592\ Z) \quad (1)$$

where X, Y, and Z are tristimulus values with illuminant C and observer 2°.

The difference of total color (ΔE) was calculated following Eq. (2):

$$\Delta E = (\Delta L^* + \Delta a^* + \Delta b^*)^{1/2} \quad (2)$$

$$\Delta L^* = L^* - Lo^*; \Delta a^* = a^* - ao^*; \Delta b^* = b^* - bo^*$$

where L_o*, a_o*, and b_o* are the corresponding to control systems (C or CNANI) parameters and L^*, a^*, and b^* are the parameters of the different systems evaluated.

- Water vapor permeability (WVP) was determined gravimetrically at 25 ºC according to ASTM E96-00 (2000) procedure (Ollé Resa et al., 2014).
- Moisture content was determined as described in "Physicochemical Characterization of Processed Rice Bran."
- Solubility in water (SW) was determined according to Flores et al. (2007).

- Mechanical testing was performed using an Instron Universal Testing Machine model 3345 (Instron Ltd., USA) working in a tensile mode. Previously, sample thickness was measured using a digital micrometer (Mitutoyo, Japan), at three different positions. Tested filmstrips (60 mm × 6 mm) were mounted between pneumatic grips with an initial separation of 20 mm. The crosshead speed applied was 0.8 mm s^{-1}. Tensile force (N) versus displacement (mm) curves was registered with the Blue Hill 2.0 software (Instron Ltd., USA). The strength and the strain at break, as well as the Young's modulus, were calculated according to Ollé Resa et al. (2014). Additionally, the following parameters for composite materials were obtained according to Shia and Hui (1998): $\left(\frac{l}{h}\right)_c = \frac{\sigma_{fu}}{2\tau_y}$ that relates the length (l) and the thickness (h) ratio of platelet fiber with the interfacial strength (τ_y, MPa) and the fiber ultimate tensile strength (σ_{fu}, MPa). A critical ratio, $\left(\frac{l}{h}\right)_c$, corresponds to its maximum value for which the maximum allowable stress can be achieved for a given load. This parameter is determined by the composite properties (filler and matrix) and the interactions in the fiber–matrix interface. From literature data, the σ_{fu} was obtained (Chen et al., 2018) while τ_y was estimated as the $\sigma_m/2$ (σ_m, ultimate tensile strength of matrix).
- Fourier transform infrared spectroscopy (FTIR). A spectrometer (V5.3.1 Spectrum, Perkin Elmer Inc., USA) provided with an Attenuated Total Reflection accessory was used. The FTIR spectra were obtained between 400 and 4000 cm^{-1} (resolution of 2 cm^{-1}).
- Microscopic observation: Optical microscopy (Olympus BX43, Japan) and scanning electron microscopy (SEM) was carried out in order to study the morphology of film surface and the cross-section (Ollé Resa et al., 2014).

Diffusion Test

The antimicrobials diffusion to a semi-solid medium was evaluated. Previously, a mixed culture was prepared with yeast *Saccharomyces cerevisiae* (CBS 1171) and bacteria gram-positive *Listeria innocua* (CIP 80.11) at 28 ºC (Berti et al., 2020). The yeast reduces the shelf-life, causes an undesirable flavor, and affects visual appearance. While the bacteria is used as a surrogate of *Listeria monocytogenes* (Pinto et al., 2011), a pathogenic bacteria that it is a public health problem since it produces listeriosis. Both microorganisms are representative of common spoilage and pathogenic microorganisms present in food. An inoculum of 1 mL was dispensed onto Plate Count Agar (Biokar Diagnostics) plates and distributed on the entire surface. Subsequently, 0.7-cm-diameter disks of antimicrobial films were placed in contact with the inoculated agar. Additionally, a film without antimicrobials was analyzed as a control system. The plates were stored at 4 °C for 48 h and then incubated at 28 °C for 24–48 h. The antimicrobial effectiveness was determined by the presence of clear zones (halos) due to growth inhibition around the disks.

Statistical Analysis of Data

Data were analyzed for differences through one-way ANOVA. Significance level ($p < 0.05$) and the Tukey *post hoc* test were applied. Results are reported based on their mean and standard deviation. The software InfoStat version 2020 (Centro de Transferencia InfoStat, FCA, Universidad Nacional de Córdoba, Argentina) was used for data analysis.

Results and Discussion

Physicochemical Characterization of Processed Rice Bran

Proximate Analysis

According to the proximate analysis of the PRB (Table 2), the insoluble dietary fiber was the main component observed. From rice composition data reported in bibliography, the insoluble fiber content in the bran is around 22-30% w/w (Kalpanadevi et al., 2018). Because of the bran preparation in the present work, soluble components (sugars, proteins, and gelatinized starch) could be lost, obtaining a product with increased fiber content.

Size Particle Distribution and Morphology

The PRB size particle distribution after sieving is shown in Fig. 1a. It was observed an asymmetrical distribution where d(0.1), d(0.5) and d(0.9) diameters were 26 µm, 77 µm, and 151 µm, respectively. The different values obtained for D[3,2] (46 µm) and D[4,3] (84 µm) indicated heterogeneity in sizes and shapes of particles. According to the mesh size used to bran separation, particles should be lower than 105 µm. Probably,

Table 2 Proximate analysis of processed rice bran

Component	g 100 g^{-1} sample (wet base)
Moisture	6.50 ± 0.05
Ash	8.1 ± 0.2
Protein	7.7 ± 0.5
Fiber	34.0 ± 0.6
Lipids	17.2 ± 0.3
Carbohydrates	26.5 ± 2.0

Shown values are an average ($n = 3$) and the corresponding standard deviation

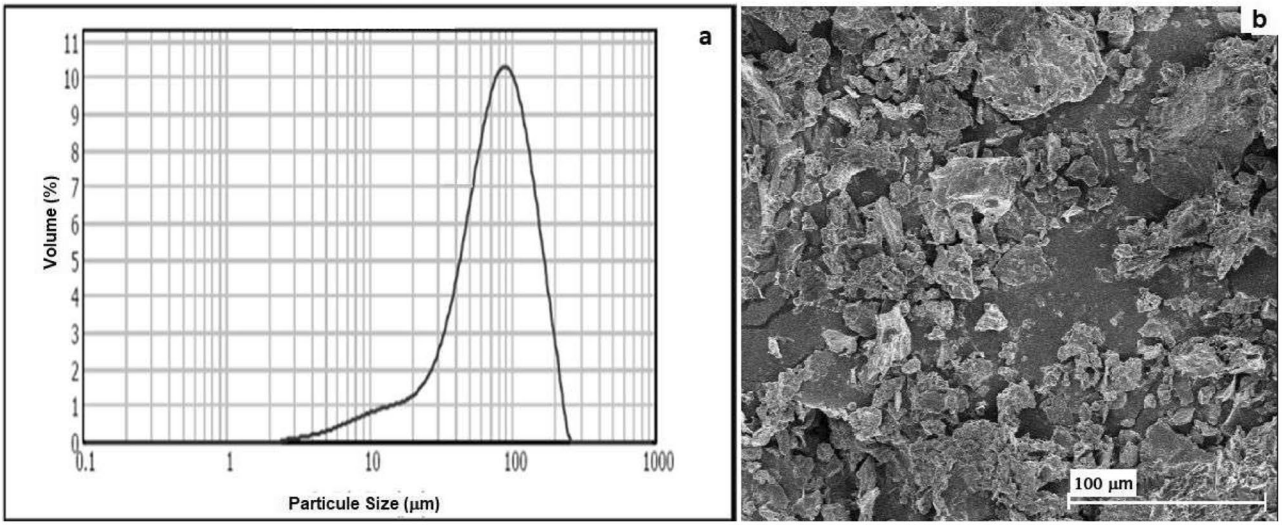

Fig. 1 **a** Size particle distribution of processed rice bran obtaining by static light scattering and **b** micrograph of rice bran by scanning electron microscopy (bar 100 μm)

aggregation or swelling of bran particles in aqueous media could be happen and therefore a little fraction of particles showed higher sizes values by static light scattering. Additionally, the frequency of different size particles was determined. Results indicated that small particles (<10 μm) were 89% by number whereas only 11% ranged between 10 and 180 μm.

The morphology of PRB can be seen in Fig. 1b. Irregular shapes with high proportion of plate-like and jagged particles were detected. Most of the particles had a length lower 20 μm correlating well with static light scattering results. Image analysis (ImageJ 1.53a Wayne Rasband, USA) of micrographs allowed estimating an aspect ratio (length/thickness) of bran particles around 7.2.

Physicochemical Characterization of Films

Color Evaluation

The color parameters of films are shown in Table 3. It could be observed that the control system (C) had the highest L* and a* but the lowest b* and YI, in comparison with S1, S2, and S3. Moreover, films showed an important increase of b* and YI and a moderate but significant reduction of L* and a*, as PRB concentration was higher determining that the addition of the filler darkened the plain film matrix. It is important to remark that the acceptability of the consumer will depend on the changes produced in the food natural coloration due to the application of the film.

When NANI was added to starch matrix (CNANI), a significant increase in yellow color (b* and YI) was observed in relation to C. Furthermore, systems with bran and antimicrobials (SNANI1, SNANI2, and SNANI3) had higher values of b*, YI, and a* than CNANI and PRB-free films. Apparently, the own color of PRB and NANI significantly browned the films, being such effect proportionally to fiber concentrations. Accordingly, a significant increase in ΔE value for higher amounts of PRB was observed, mainly due to the increase of b*. Robles-Flores et al. (2018) observed L* values close to 55 in films and edible coatings obtained from the *Cajanus cajan* seed (protein isolate and gum) applied

Table 3 Color parameters of films containing different processed rice bran concentrations (S1, S2, and S3), containing antimicrobials and different rice bran concentrations (SNANI1, SNANI2, and SNANI3) and control films (C, CNANI)

	L*	a*	b*	YI	ΔE
C	88 ± 1 b	−1.18 ± 0.06 a	3.7 ± 0.3 a	6.7 ± 0.5 a	–
S1	86.8 ± 0.4 a	−1.39 ± 0.05 b	5.5 ± 0.5 b	10.4 ± 0.8 b	2.2 ± 0.2 a
S2	87.1 ± 0.7 a	−1.60 ± 0.02 c	6.9 ± 0.2 c	12.8 ± 0.7 c	3.4 ± 0.4 b
S3	86.5 ± 0.6 a	−1.62 ± 0.03 c	8.2 ± 0.6 d	15 ± 1 d	4.8 ± 0.2 c
CNANI	87.7 ± 0.5 B	−1.23 ± 0.09 A	9.74 ± 0.04 A	18.4 ± 0.5 A	–
SNANI1	86.3 ± 0.2 AB	−1.2 ± 0.2 AB	13.0 ± 0.6 B	23 ± 1 B	3.5 ± 0.4 A
SNANI2	86.1 ± 0.7 AB	−1.17 ± 0.06 B	12.9 ± 0.8 B	25 ± 2 B	3.5 ± 0.4 A
SNANI3	85.0 ± 0.2 A	−0.7 ± 0.1 B	15.1 ± 0.8 B	29 ± 2 B	6.0 ± 0.4 B

Mean and standard deviation are reported ($n = 4$). Different lowercase letters in the same column indicate significant differences ($p < 0.05$) among systems without antimicrobials. Different capital letters in the same column indicate significant differences ($p < 0.05$) among systems with antimicrobials.

L*, a* and b* are defined in Physicochemical Characterization of Films

to fresh strawberry fruit, reporting that the application of edible coating did not affect the strawberries appearance. Somboonsub and Thawornchinsombut (2015) also observed an L* decrease (91.52 to 86.68) but higher a* and b* values (0.41 to 1.78 and 9.11 to 12.42, respectively), when rice bran protein was incorporated from 0 to 30 g g^{-1} starch to cassava starch films.

Water Vapor Permeability

Water vapor permeability results are shown in Table 4. It was observed that films with different concentrations of PRB added or not with antimicrobials did not show significant differences in WVP being the mean value $(1.6 \pm 0.2) \times 10^{-9}$ g m^{-1} s^{-1} Pa^{-1}. Considering the starch-base matrix, the barrier property of studied films agree with those reported by Flores et al. (2007) for tapioca starch:glycerol edible films, $(1.4 \pm 0.2) \times 10^{-9}$ g m^{-1} s^{-1} Pa^{-1}, and by Famá et al. (2009), $(5.5 \pm 0.1) \times 10^{-10}$ g m^{-1} s^{-1} Pa^{-1}, for starch-based films plasticized with glycerol and added with 0.15% w/w of wheat bran. Other authors (Bernhardt et al., 2017), studying the effect of a filler in the matrix, observed a decrease in WVP when corn husk fiber was added to pectin-based films, reporting values around 9×10^{-10} g m^{-1} s^{-1} Pa^{-1} for systems with 3–8% w/w fiber in comparison with the control without filler (1×10^{-9} g m^{-1} s^{-1} Pa^{-1}). Moreover, Ollé Resa et al. (2014) reported that NANI incorporation in a starch matrix did not modify the WVP. The authors registered a WVP of $(1.89 \pm 0.07) \times 10^{-9}$ g m^{-1} s^{-1} Pa^{-1} and $(1.03 \pm 0.07) \times 10^{-9}$ g m^{-1} s^{-1} Pa^{-1} for films without or with NANI, respectively. Even though the filler addition to film matrix supposes a reduction of the vapor transmission rate, because of the higher tortuosity of the pathway, other factors must be considered. It was established that the influence of fillers on biobased films permeability depends on biopolymer structure, filler concentration, type, and their compatibility with the network (Versino & Garcia, 2014). Probably, in the present research, the PRB incorporated to films formulation was not enough to modify the water barrier property significantly.

Table 4 WVP and water solubility of films with different concentrations of processed rice bran (S1, S2, and S3), control film (C), and films with natamycin, nisin, and different concentrations of processed rice bran (CNANI, SNANI1, SNANI2, SNANI3)

	WVP × 10^9 (g m^{-1} s^{-1} Pa^{-1})	Solubility in water (%)
C	1.6 ± 0.3 a	34.6 ± 0.9 a
S1	1.4 ± 0.2 a	26 ± 2 b
S2	1.5 ± 0.2 a	25 ± 2 b
S3	1.7 ± 0.3 a	35 ± 2 a
CNANI	1.9 ± 0.8 A	40.0 ± 0.7 B
SNANI1	1.7 ± 0.1 A	41.6 ± 0.5 B
SNANI2	2.0 ± 0.2 A	37.8 ± 0.7 A
SNANI3	1.3 ± 0.3 A	42.3 ± 0.1 B

Mean and standard deviation are reported ($n = 2$). Different letters indicate significant differences ($p < 0.05$) in the same column

Solubility in Water

It is observed in Table 4 that the addition of PRB in S1 and S2 decreased the films SW around ≈26% with respect to C. A more water-resistant film structure could be the result of a strong adhesion between filler and starch matrix. However, SW of S3 was similar to control C. In this case, such PRB level could have disrupted the starch network which becomes more susceptible to water as a solvent. Edhirej et al. (2017) observed similar effects in relation to cassava/sugar palm fiber addition to cassava starch–based composites.

The antimicrobials' presence increased, in general, the SW of films. In a previous report, Ollé Resa et al. (2014) observed a plasticizer action of preservatives (NANI) which reduced the interactions of biopolymer chains in the matrix producing a more soluble film. However, a significant lower solubility of SNANI2 was observed, indicating an improvement in water resistance, maybe due to a better interaction and compatibility among film components.

Mechanical Properties

The developed films were flexible, were easy to handle, and had an average thickness of 0.27 ± 0.04 mm ($n = 12$). The results of tensile strength, Young's modulus, and strain at break of studied films are shown in Fig. 2.

An increase in tensile strength was observed for S2 (1.9 ± 0.2 MPa) in comparison with C, S1, and S3. In addition, Young's modulus was minimal for S1 but non-significant differences ($p > 0.05$) were observed for C, S2, and S3. Regarding strain at break, the highest value was obtained for S2 (1.35 ± 0.08). It could be established that the major factors that modulate the properties of fiber–starch composites are related to fiber volume fraction, dispersion, size, shape, orientation, and fiber–matrix adhesion (Gutiérrez & Alvarez, 2017). As was previously determined, the particle size distribution of PRB showed a major proportion of small particles (<10 μm). Such fraction was probably better covered by the matrix and well separated from each other in all samples; therefore, the stress could be transferred more effectively to the whole composite. Contrarily, large particles (10–180 μm) might be hardly lodged as bran concentration was increased. According to tensile strength results, the higher efficiency of the filler was obtained for S2, indicating a more effective adhesion and evenly distribution of the stress. Below 0.2%, the amount of fiber incorporated was not enough to modify the tensile

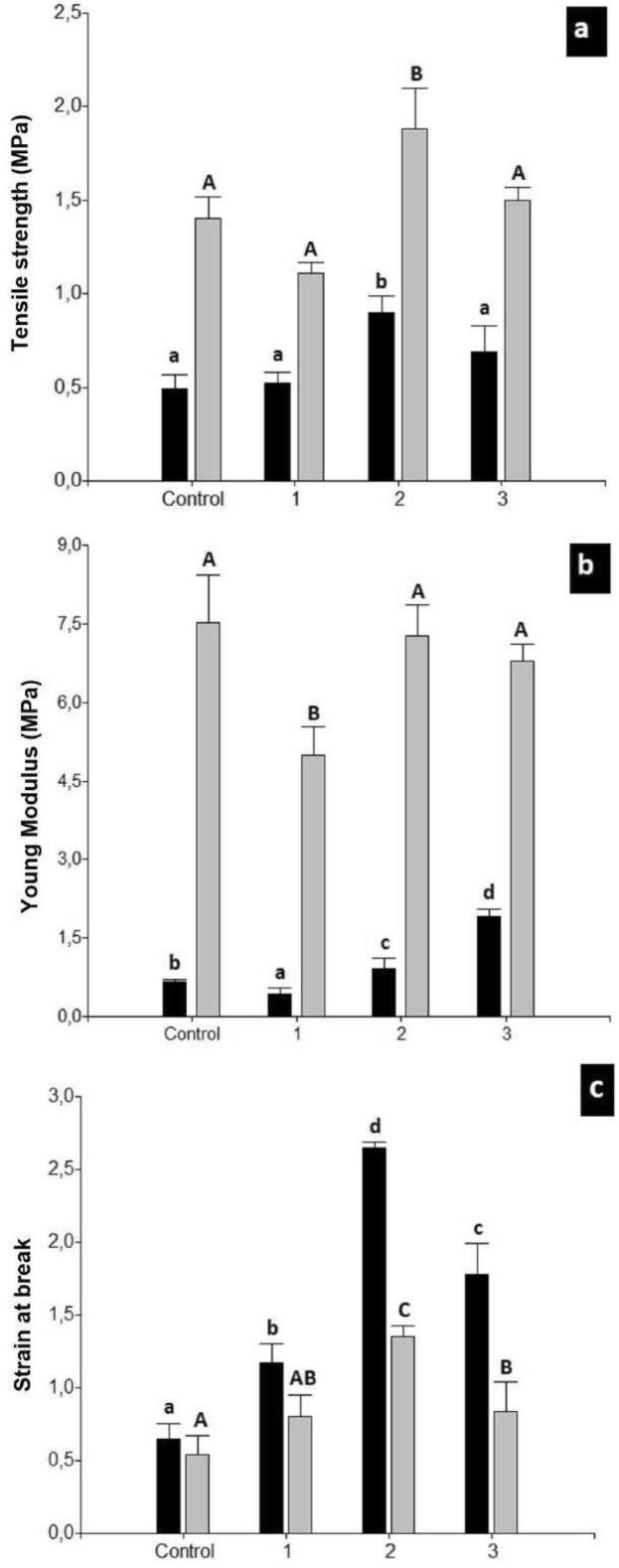

Fig. 2 Mechanical properties of films: tensile strength at break (**a**), Young's modulus (**b**), and strain at break (**c**). Numbers 1, 2, and 3 indicate 0.1, 0.2, and 0.3 g processed rice bran 100 g^{-1} slurry, respectively. Gray and black bars represent films without or with natamycin and nisin, respectively. Different letters indicate significant differences among films ($p < 0.05$)

strength significantly. On the other hand, the matrix could not be able to properly support the bran particles in S3 films, especially the big ones, promoting poor distribution and flocculation that reduced the reinforcing capacity of PRB. It was reported that a plain reinforcement effect of fiber is commonly observed until a maximum, which is determined by the filler tendency to agglomerate or break through the matrix, triggers the weakening of the film structure (Kaewtatip & Thongmee, 2012). Kargarzadeh et al. (2017) observed similar effects when incorporating different amounts of cellulose nanocrystals from rice husk fiber to starch matrix. The starch biocomposites with 6% d.b. of cellulose nanocrystals showed the highest tensile strength with an improvement of 52%, while the addition of a higher percent, 8 and 10%, presented lower values. In the same way, they observed that the deformation and Young's modulus were maximum with the addition of 6% and then decreased with 8 and 10%.

Besides, $\left(\frac{l}{h}\right)_c$ was expected in the range of 14–97 and compared with the aspect ratio of PRB used herein (≈7.2), showing that the maximum filler stress was not reached for the studied systems and, consequently, the plain reinforcement capacity of the bran was not fully exploited. Probably, in S2 film the higher amount of filler could have compensated, in part, the low aspect ratio obtained for PRB.

Otherwise, when NANI was added to film formulation, tensile strength, and Young's modulus were diminished in all systems, which could be attributed to the plasticizer effect of antimicrobials on starch matrix, as was previously reported (Ollé Resa et al., 2014). Additionally, Shiroodi et al. (2016) showed significant reductions in mechanical properties of polylactic acid–based films containing nisin compared to control films without antimicrobial.

In the present research, besides the NANI presence, the reinforcing trend of PRB incorporation was also observed (Fig. 2a, b). Accordingly, SNANI2 showed the highest tensile strength parameter. In general, tensile strength and Young's modulus decreases (55% and 85% respectively) were observed for all systems with NANI in comparison with films without antimicrobials. In contrast, the combined presence of NANI and PRB produced a significant increase of strain at break (Fig. 2c). Contrarily, Ge et al. (2017) reported an increase in tensile strength and Young's modulus but a decrease in strain at break with increase in the concentration of amino-functionalized montmorillonite (filler) in gelatin-based edible films containing nisin.

In order to further characterize the developed films, S2 and SNANI2 were selected regarding their better mechanical properties and SW. In addition, C and CNANI or S1 and S3 systems were analyzed for comparison reasons.

Fourier Transform Infrared Spectroscopy

The FTIR spectra of C, S2, CNANI, and SNANI2 films are shown in Fig. 3 where the typical bands of starch matrix, as main component of film formulation, were observed: a broad band around 3300 cm^{-1} related to the stretching of the O–H groups free or linked by means of intra- and intermolecular hydrogen bonds, a peak around 2930 cm^{-1} assigned to the C–H bond stretch, a signal at 1650 cm^{-1} linked to the O–H flexing of the water in the starch (water bound to the structure), and the bands in the range from 1300 to 900 cm^{-1} associated to C–O and C–C stretching bonds of the anhydroglucose ring, with this zone being more sensitive to molecular conformation (Vicentini et al., 2005). It is possible to appreciate that the 1650-cm^{-1} band (bound water) had a different intensity depending on the film sample. Therefore, the absorbance ratio 1650 cm^{-1}/1455 cm^{-1} (CH_2 bending in plane) was calculated to predict the level of water present in film matrix, showing that CNANI (0.899) > SNANI2 (0.655) > C (0.362) >> S2 (0.019). Apparently, films containing S2 excluded some water molecules from the film network, possibly in the interphase zone, due to a good compatibility between PRB and starch through hydrophilic groups. Contrarily, CNANI seemed to develop the major water–starch interactions while SNANI2 trended to replace some of these with PRB–starch matrix bonds. Edhirej et al. (2017) reported that cassava starch film showed an intense signal at 1658 cm^{-1}, but this band decreased gradually and proportionally as the amount of sugar palm fiber increased. The observed trends in the intensity of 1650 cm^{-1} band in the present research can be related with the moisture content of films: 30.3 ± 0.1, 34.39 ± 0.05, 15.7 ± 0.2, and 13.5 ± 0.3 g/100 g w.b. for CNANI, SNANI2, C, and S2, respectively. Effectively, S2 film showed the lowest moisture value ($p < 0.05$) while NANI presence could promote the establishment of more layers of absorbed water, possibly due to its plasticizer effect that imparts a higher hydrophilic character of such films as was previously explained in SW results ("Solubility in water"). The determined moisture levels and the known water plasticizer effect could partially explain the strain at break increase of SNANI2 in relation to S2 and CNANI and C films (Fig. 2c).

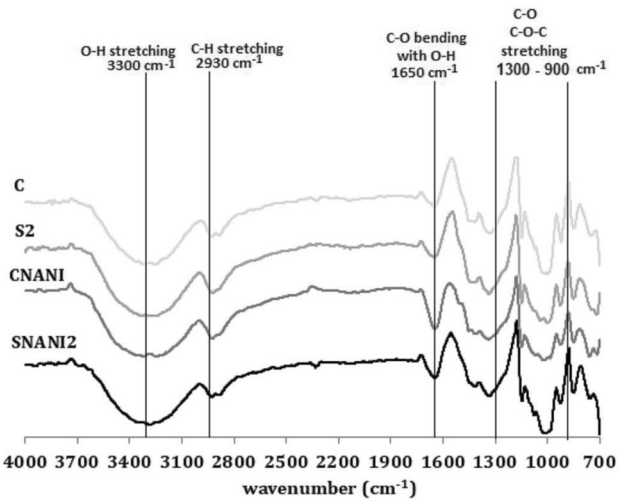

Fig. 3 Fourier transform infrared spectroscopy (FTIR) spectra of starch-based films: control (C), with 0.2 g of processed rice bran (S2), with natamycin and nisin (CNANI), and with 0.2 g of processed rice bran, natamycin, and nisin (SNANI2)

Several authors (Monroy et al., 2018; Wang et al., 2015) have reported the 1047 cm^{-1}/1022 cm^{-1} and 1022 cm^{-1}/995 cm^{-1} absorbance ratios as indicators of ordered-to-amorphous and amorphous-to-hydrated starch structures, respectively. On increase of starch structure organization, the first mentioned ratio increases while the second one decreases (Ambigaipalan et al., 2013; Monroy et al., 2018). The calculated 1047 cm^{-1}/1022 cm^{-1} ratios were S2 (1.098) > C (0.627) > SNANI2 (0.595) > CNANI (0.444) while 1022 cm^{-1}/995 cm^{-1} ratios were CNANI (1.936) > SNANI2 (1.068) > C (1.007) > S2 (0.675), suggesting that S2 films presented the more organized matrix structure while antimicrobial presence, contrarily, increased the amorphous character. The plasticizer action of natural preservatives was the main reason for SNANI2 and CNANI 1022 cm^{-1}/995 cm^{-1} ratios. It was reported that an increase in the crystalline phase of a semi-crystalline material is highly linked with the decrease in its moisture content (Famá et al., 2009). Such trend could have contributed to the observed reduction in the moisture content of S2 and C films in comparison with antimicrobial films. In addition, the increase of organized structures in a plasticized starch matrix when a cellulosic fiber is added has been linked to a facilitated ability of amylopectin chains to crystallize in the filler-starch interphase zone (Angle`s & Dufresne, 2000). Probably, such a condition could have collaborated in the development of a higher tensile strength response of S2 films in comparison with C, CNANI, and SNANI2 films (Fig. 2a).

Microstructure: Optical Microscopy and SEM

Images observed under the optical microscope showed a homogeneous and continuous matrix for C films (Fig. 4a) while variable shapes and a uniform PRB distribution in a clear matrix could be observed for S1 and S2 (Fig. 4b, c). When a higher amount of PRB was used (S3, Fig. 4d), particle density increased, darkening the matrix in agreement with color results (Table 3). According to Ludueña et al. (2012), the increase of filler density into matrix could promote the aggregate constitution. The presence of these clusters does not allow correct matrix–filler interaction, and therefore a weaker polymer-filler interfacial adhesion than expected is obtained. Regarding such phenomenon, SW and mechanical results observed for S3 could be explained.

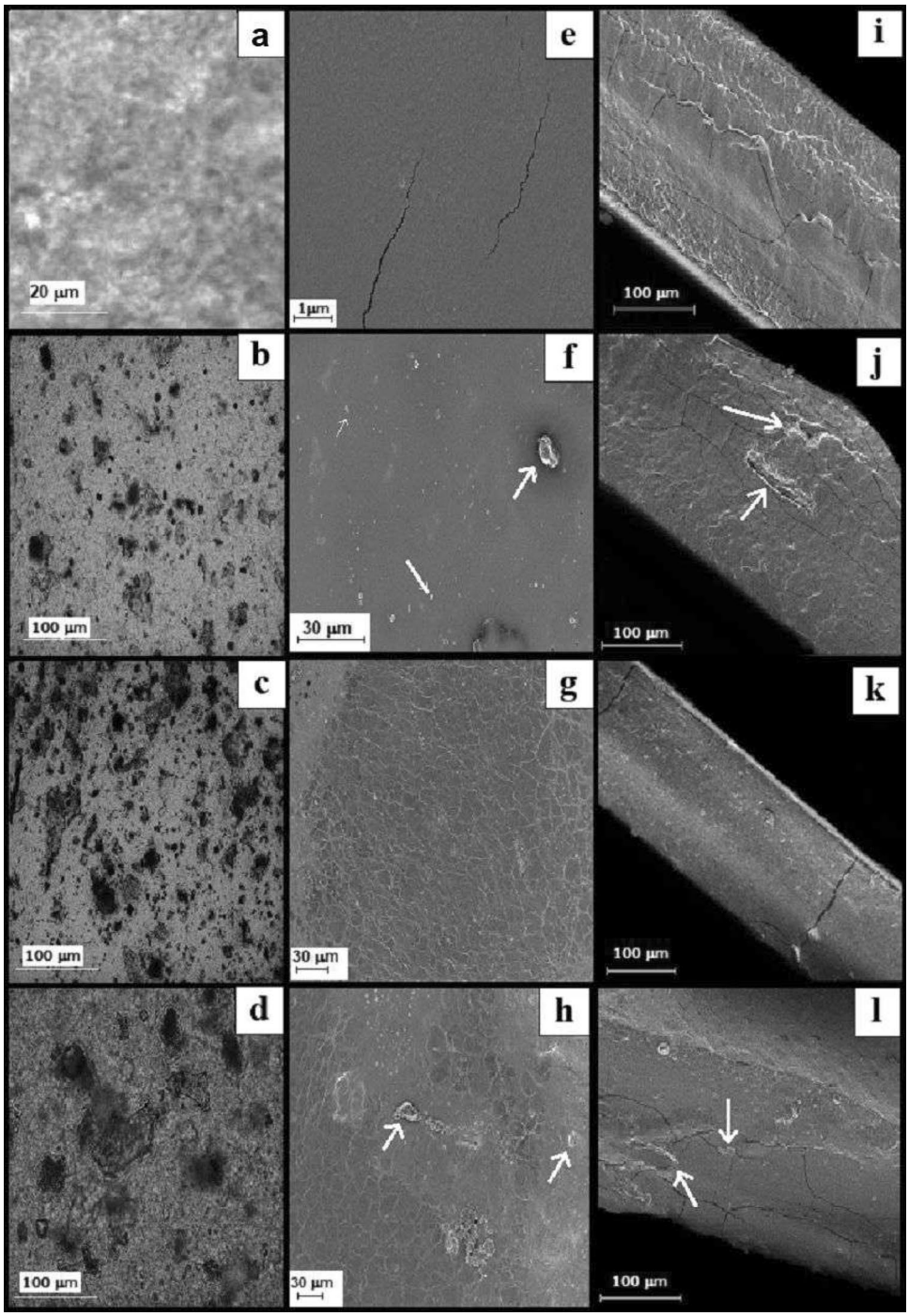

Fig. 4 Optical microscopy of C (control film) (**a**) and films with 0.1 g (**b**), 0.2 g (**c**), and 0.3 g (**d**) of processed rice bran 100 g^{-1} slurry. Scanning electron microscopy micrographs (SEM) of surfaces of C (**e**), S2 (**f**), CNANI (**g**), and SNANI2 (**h**) films. SEM images of fractured surfaces C (**i**), S2 (**j**), CNANI (**k**), and SNANI2 (**l**) films. The arrows indicate processed rice bran particles into the matrix

SEM was used to qualitatively examine the microstructure and the interfacial adhesion of starch matrix and PRB. The C films showed a homogeneous surface (Fig. 4e) while CNANI exhibited a lattice-like and continuous structure (Fig. 4g). Both films had a compact assembly (Fig. 4i-k), and some natamycin fragments evenly incorporated into matrix were observed in CNANI.

The addition of the filler in S2 and SNANI2 (Fig. 4f-h) led to the formation of a more heterogeneous surface with some filler particles exposed on the surface (pointed out with arrows in Fig. 4f-h).

The micrographs of the fracture surface of S2 and SNANI2 (Fig. 4j-l) revealed that the PRB was tightly covered with a dense starch matrix, being structurally incorporated in the network. In addition, no holes or empty spaces were observed around the PRB–matrix interface, suggesting strong interaction between both components. It was reported that natural fillers and starch networks could have high chemical compatibility

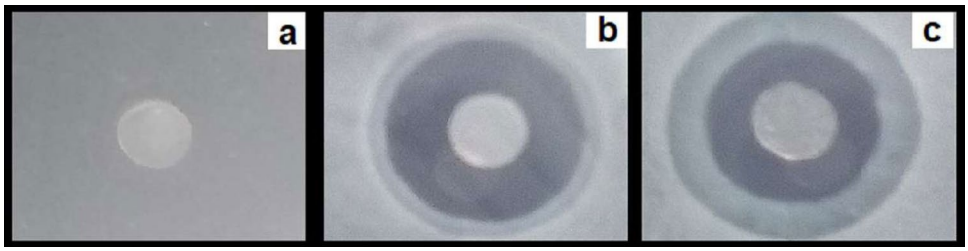

Fig. 5 Diffusion test results of films: with 0.2 g of processed rice bran 100 g^{-1} slurry (**a**), with natamycin and nisin (**b**) and with 0.2 g of processed rice bran, natamycin, and nisin (**c**), against *Saccharomyces cerevisiae* and *Listeria innocua* mixture culture

and good adhesion in the interfacial zone due to their hydrophilic character (Kuciel & Liber-Knec, 2009). Similar observations have been reported by other authors for starch-based composites (Edhirej et al., 2017; Fu et al., 2017; Kargarzadeh et al., 2017). Moreover, a more integrated network structure in film SNANI2 than S2 was observed, suggesting an improvement in the compatibility of film components when NANI was present.

Diffusion Test

The results of the diffusion test performed in semi-solid medium for S2, CNANI, and SNANI2 are shown in Fig. 5a-c respectively. The film with rice bran and without antimicrobial (S2) did not allow the formation of halos, showing that this film did not present antimicrobial properties (Fig. 5a). On the other hand, an internal inhibition halo is observed in Fig. 5b, c which corresponds to the *L. innocua* inhibition zone by action of nisin, and an external halo that corresponds to the *S. cerevisiae* inhibition zone by action of natamycin. The diameters of the halos were CNANI: 2.5 ± 0.1 cm and SNANI2: 2.1 ± 0.1 cm for natamycin, and CNANI: 2.1 ± 0.1 cm and SNANI2: 1.7 ± 0.1 cm for nisin. Although a significantly ($p < 0.05$) lower halo was observed for *L. innocua* in SNANI2 than in CNANI, it was verified that the PRB incorporated (Fig. 5c) did not prevent the diffusion of NANI, allowing the formation of inhibition halos for yeast and bacteria effectively.

Pintado et al. (2010) observed the formation of halos with a similar size in whey protein films containing malic acid, nisin, and natamycin, against spoilage (*Yarrowia lipolytica* and *Penicillium roqueforti*) and pathogenic microorganism (*L. monocytogenes* and *Pseudomonas aeruginosa*) isolated from cheese surface. Additionally, Resa et al. (2014) observed similar double halos in starch-based film with natamycin and nisin and verified that the smallest corresponded to the inhibition of growth of *L. innocua* and the biggest to the one of *S. cerevisiae*.

Conclusions

It was possible to develop and characterize an edible film based on tapioca starch supporting the natural antimicrobials natamycin and nisin (NANI) and reinforced with processed rice bran (PRB). The influence of PRB presence on film properties such as color, solubility in water (SW), mechanical response and the composite structure was established.

This research showed that the incorporation of 0.2% of PRB to films without antimicrobials (S2) increased the yellowness, maximized tensile strength, and strain at break and reduced the SW, compared with control film (C). The addition of NANI reduced the tensile strength and Young modulus and increased SW in all formulations. In addition, in the antimicrobial film (SNANI2), NANI was available to diffuse in a semi-solid medium and showed an effective action against *S. cerevisiae* and *L. innocua*.

It was proven that agro-waste-based filler addition to starch-based films containing NANI enhanced mechanical and SW properties and maintained the antimicrobial protection. Therefore, these results present an ecological approach to develop biocomposite films that can be used as active packaging material for food preservation.

Acknowledgements The authors wish to thank DSM (Argentina) and Cooperativa Arrocera Villa Elisa (Entre Ríos, Argentina).

Author Contribution Sofía Berti: investigation, methodology, formal analysis, data curation, validation, writing—original draft, visualization. Rosa J Jagus: conceptualization, methodology, resources, investigation, formal analysis, validation, visualization, supervision, project administration, funding acquisition, writing—original draft, writing—review and editing. Silvia K Flores: conceptualization, methodology, resources, formal analysis, investigation, visualization, supervision, project administration, funding acquisition, writing—original draft, writing—review and editing.

Funding This study was financially supported by Universidad de Buenos Aires (UBACyT 2002017010063BA, 2017–2020, and UBACyT 20020130100550BA, 2014–2017), Agencia Nacional de Promoción Científica y Tecnológica (PICT 2015 No. 2742 and PICT 2015 No. 2109).

Availability of Data and Materials The authors confirm that the data supporting the findings of this study are available within the article.

Code Availability The software InfoStat version 2020 was used for statistical analysis (Centro de Transferencia InfoStat, FCA, Universidad Nacional de Córdoba, Argentina).

Declarations

Conflict of Interest The authors declare no competing interests.

References

Alzate, P., Miramont, S., Flores, S., & Gerschenson, L. (2017). Effect of the potassium sorbate and carvacrol addition on the properties and antimicrobial activity of tapioca starch – Hydroxypropyl methylcellulose edible films. *Starch/Staerke, 69*(5–6), 1–9. https://doi.org/10.1002/star.201600261

Ambigaipalan, P., Hoover, R., Donner, E., & Liu, Q. (2013). Retrogradation characteristics of pulse starches. *Food Research International, 54*(1), 203–212. https://doi.org/10.1016/j.foodres.2013.06.012

Angles, M. N., & Dufresne, A. (2000). Plasticized starch/tunicin whiskers nanocomposites. 1. *Structural analysis. Macromolecules, 33*(22), 8344–8353. https://doi.org/10.1021/ma0008701

AOAC 991.42. (1998). Official methods of analysis 15 Association of Official Analytical Chemists.

AOAC 934.01, 942.05 & 960.39. (2005). Official methods of analysis 18 Association of Official Analytical Chemists.

ASTM D1925. (1988). Standard Test Method for Yellowness Index of Plastics. Philadelphia: American Society for Testing and Materials.

ASTM E96-00. (2000). Standard test method for water vapour transmission of materials. American Society for Testing and Materials, Philadelphia (2000).

Avérous, L., & Halley, P. J. (2009). Biocomposites based on plasticized starch. *Biofuels, Bioproducts and Biorefining, 3*(3), 329–343. https://doi.org/10.1002/bbb.135

Basch, C. Y., Jagus, R. J., & Flores, S. K. (2013). Physical and antimicrobial properties of tapioca starch-HPMC edible films incorporated with nisin and/or potassium sorbate. *Food and Bioprocess Technology, 6*(9), 2419–2428.

Bernhardt, D. C., Pérez, C. D., Fissore, E. N., & De'Nobili, M. D., & Rojas, A. M. (2017). Pectin-based composite film: Effect of corn husk fiber concentration on their properties. *Carbohydrate Polymers, 164*, 13–22.

Berti, S., Flores, S. K., & Jagus, R. J. (2020). Improvement of the microbiological quality of Argentinian Port Salut cheese by applying starch-based films and coatings reinforced with rice bran and containing natural antimicrobials. *Journal of Food Processing and Preservation*, e14827. https://doi.org/10.1111/jfpp.14827

Cano, A., Jiménez, A., Cháfer, M., Gónzalez, C., & Chiralt, A. (2014). Effect of amylose:amylopectin ratio and rice bran addition on starch films properties. *Carbohydrate Polymers, 111*, 543–555. https://doi.org/10.1016/j.carbpol.2014.04.075

Cerqueira, M., Lima, A., Souza, B., Teixeira, J., Moreira, R., & Vicente, A. (2009). Functional polysaccharides as edible coatings for cheese. *Journal of Agricultural and Food Chemistry, 57*(4), 1456–1462. https://doi.org/10.1021/jf802726d

Chen, Y., Liu, C., Chang, P., Cao, X., & Anderson, D. (2009). Bionanocomposites based on pea starch and cellulose nanowhiskers hydrolyzed from pea hull fiber: Effect of hydrolysis time. *Carbohydrate Polymers, 76*(4), 607–615. https://doi.org/10.1016/j.carbpol.2008.11.030

Chen, Z., Xu, Y., & Shivkumar, S. (2018). Microstructure and tensile properties of various varieties of rice husk. *J. Sci. Food Agric, 98*, 1061–1070. https://doi.org/10.1002/jsfa.8556

Costa, M. J., Maciel, L. C., Teixeira, J. A., Vicente, A. A., & Cerqueira, M. A. (2018). Use of edible films and coatings in cheese preservation: Opportunities and challenges. *Food Research International, 107*, 84–92. https://doi.org/10.1016/j.foodres.2018.02.013

Daybelis, I., Valdés, F., Silvia, D., Baños, B., Dayvis, I., & Valdés, F. (2015). Películas y recubrimientos comestibles: una alternativa favorable en la conservación poscosecha de frutas y hortalizas. *24*(3), 52–57. ISSN 2071-0054

Edhirej, A., Sapuan, S., Jawaid, M., & Zahari, N. (2017). Cassava/sugar palm fiber reinforced cassava starch hybrid composites: Physical, thermal and structural properties. *International Journal of Biological Macromolecules, 101*, 75–83. https://doi.org/10.1016/j.ijbiomac.2017.03.045

Famá, L., Gerschenson, L., & Goyanes, S. (2009). Starch-vegetable fibre composites to protect food products. *Carbohydrate polymers, 75*(2), 230–235. https://doi.org/10.1016/j.carbpol.2008.06.018

Flores, S., Famá, L., Rojas, A. M., Goyanes, S., & Gerschenson, L. (2007). Physical properties of tapioca-starch edible films: Influence of filmmaking and potassium sorbate. *Food Research International, 40*(2), 257–265. https://doi.org/10.1016/j.foodres.2006.02.004

Fu, Z., Wu, M., Han, X., & Xu, L. (2017). Effect of okara dietary fiber on the properties of starch-based films. *Starch/Staerke, 69*(11–12), 1–7. https://doi.org/10.1002/star.201700053

Ge, L., Zhu, M., Xu, Y., Li, X., Li, D., & Mu, C. (2017). Development of antimicrobial and controlled biodegradable gelatin-based edible films containing nisin and amino-functionalized montmorillonite. *Food and Bioprocess Technology, 10*(9), 1727–1736.

Gilfillan, W., Nguyen, D., Sopade, P., & Doherty, W. (2012). Preparation and characterisation of composites from starch and sugar cane fiber. *Industrial Crops and Products, 40*, 45–54. https://doi.org/10.1016/j.indcrop.2012.02.036

Gutiérrez, T., & Alvarez, V. (2017). Cellulosic materials as natural fillers in starch-containing matrix-based films: A review. *Polymer Bulletin, 74*(6), 2401–2430. https://doi.org/10.1007/s00289-016-1814-0

Jiménez, A., Fabra, M., Talens, P., & Chiralt, A. (2012). Effect of re-crystallization on tensile, optical and water vapour barrier properties of corn starch films containing fatty acids. *Food Hydrocolloids, 26*(1), 302–310. https://doi.org/10.1016/j.foodhyd.2011.06.009

Kaewtatip, K., & Thongmee, J. (2012). Studies on the structure and properties of thermoplastic starch/luffa fiber composites. *Materials and Design, 40*, 314–318. https://doi.org/10.1016/j.matdes.2012.03.053ISSN0261-3069

Kalpanadevi, C., Singh, V., & Subramanian, R. (2018). Influence of milling on the nutritional composition of bran from different rice varieties. *Journal of food science and technology, 55*(6), 2259–2269. https://doi.org/10.1007/s13197-018-3143-9

Kargarzadeh, H., Johar, N., & Ahmad, I. (2017). Starch biocomposite film reinforced by multiscale rice husk fiber. *Composites Science and Technology, 151*, 147–155. https://doi.org/10.1016/j.compscitech.2017.08.018

Kuciel, S., & Liber-Knec, A. (2009). Biocomposites on the base of thermoplastic starch filled by wood and kenaf fiber. *Journal of Biobased Materials and Bioenergy, 3*(3), 269–274. https://doi.org/10.1166/jbmb.2009.1026

Lafargue, D., Lourdin, D., & Doublier, J. (2007). Film-forming properties of a modified starch/κ-carrageenan mixture in relation to its rheological behaviour. *Carbohydrate Polymers, 70*(1), 101–111. https://doi.org/10.1016/j.carbpol.2007.03.019

Lowry, O., Rosebrough, N., Farr, A., & Randall, R. (1951). Protein measurement with the Folin phenol reagent. *Journal of Biological Chemistry, 193*, 265–275.

Ludueña, L., Vázquez, A., & Alvarez, V. (2012). Effect of lignocellulosic filler type and content on the behavior of polycaprolactone based eco-composites for packaging applications. *Carbohydrate Polymers, 87*(1), 411–421. https://doi.org/10.1016/j.carbpol.2011.07.064

Monroy, Y., Rivero, S., & García, M. A. (2018). Microstructural and techno-functional properties of cassava starch modified by ultrasound. *Ultrasonics Sonochemistry, 42*, 795–804. https://doi.org/10.1016/j.ultsonch.2017.12.048

Moro, T. M., Ascheri, J. L., Ortiz, J. A., Carvalho, C. W., & Meléndez-Arévalo, A. (2017). Bioplastics of native starches reinforced with

passion fruit peel. *Food and Bioprocess Technology, 10*(10), 1798–1808.

Ollé Resa, C. P., Jagus, R. J., & Gerschenson, L. N. (2021). Do fillers improve the physicochemical properties of antimicrobial tapioca starch edible films?. *Journal of Food Safety,* e12880. https://doi.org/10.1111/jfs.12880

Ollé Resa, C., Jagus, R., & Gerschenson, L. (2014). Effect of natamycin, nisin and glycerol on the physicochemical properties, roughness and hydrophobicity of tapioca starch edible films. *Materials Science and Engineering C, 40*, 281–287. https://doi.org/10.1016/j.msec.2014.04.005

Pérez, P. F., Resa, C. P. O., Gerschenson, L. N., & Jagus, R. J. (2021). Addition of zein for the improvement of physicochemical properties of antimicrobial tapioca starch edible film. *Food and Bioprocess Technology,* 1-10.

Pintado, C. M., Ferreira, M. A., & Sousa, I. (2010). Control of pathogenic and spoilage microorganisms from cheese surface by whey protein films containing malic acid, nisin and natamycin. *Food Control, 21*(3), 240–246. https://doi.org/10.1016/j.foodcont.2009.05.017

Pinto, M. S., de Carvalho, A. F., Pires, A. C. D. S., Campos Souza, A. A., Fonseca da Silva, P. H., Sobral, D., & de Lima Santos, A. (2011). The effects of nisin on Staphylococcus aureus count and the physicochemical properties of Traditional Minas Serro cheese. *International Dairy Journal, 21*(2), 90–96. https://doi.org/10.1016/j.idairyj.2010.08.001

Prachayawarakorn, J., Chaiwatyothin, S., Mueangta, S., & Hanchana, A. (2013). Effect of jute and kapok fibers on properties of thermoplastic cassava starch composites. *Materials and Design, 47*, 309–315. https://doi.org/10.1016/j.matdes.2012.12.012

Resa, C. P. O., Gerschenson, L. N., & Jagus, R. J. (2014). Natamycin and nisin supported on starch edible films for controlling mixed culture growth on model systems and Port Salut cheese. *Food Control, 44*, 146–151. https://doi.org/10.1016/j.foodcont.2014.03.054

del C Robles-Flores, G., Abud-Archila, M., Ventura-Canseco, L. M. C., Meza-Gordillo, R., Grajales-Lagunes, A., Ruiz-Cabrera, M. A., & Gutiérrez-Miceli, F. A. (2018). Development and evaluation of a film and edible coating obtained from the Cajanus cajan seed applied to fresh strawberry fruit. *Food and Bioprocess Technology, 11*(12), 2172–2181.

Somboonsub, S., & Thawornchinsombut, S. (2015). Effect of rice bran protein and cassava starch ratio on physical, mechanical and structural properties of rice bran protein-cassava starch composite film. *Journal of Food Science and Agricultural Technology*, *1*(1), 63–67. ISSN: 2408-1736.

Shia, D., & Hui, C. Y. (1998). An interface model for the prediction of Young's modulus of layered siIicate-elastomer nanocomposites. *Polymer composites, 19*, 608–617. https://doi.org/10.1002/pc.10134

Shiroodi, S. G., Nesaei, S., Ovissipour, M., Al-Qadiri, H. M., Rasco, B., & Sablani, S. (2016). Biodegradable polymeric films incorporated with nisin: Characterization and efficiency against *Listeria monocytogenes*. *Food and Bioprocess Technology, 9*(6), 958–969.

Toro-Márquez, L. A., Merino, D., & Gutiérrez, T. J. (2018). Bionanocomposite films prepared from corn starch with and without nanopackaged Jamaica (Hibiscus sabdariffa) flower extract. *Food and Bioprocess Technology, 11*(11), 1955–1973.

Vásconez, M. B., Flores, S. K., Campos, C. A., Alvarado, J., & Gerschenson, L. N. (2009). Antimicrobial activity and physical properties of chitosan–tapioca starch based edible films and coatings. *Food Research International, 42*(7), 762–769. https://doi.org/10.1016/j.foodres.2009.02.026

Versino, F., & García, M. A. (2014). Cassava (Manihot esculenta) starch films reinforced with natural fibrous filler. *Industrial Crops & Products, 58*, 305–314. https://doi.org/10.1016/j.indcrop.2014.04.040

Vicentini, N. M., Dupuy, N., Leitzelman, M., Cereda, M. P., & Sobral, P. J. A. (2005). Prediction of cassava starch edible film properties by chemometric analysis of infrared spectra. *Spectroscopy Letters: An International Journal for Rapid Communication, 38*(6), 749–767. https://doi.org/10.1080/00387010500316080

Wan, J., Liu, C., Liu, W., Tu, Z., Wu, W., & Tan, H. (2015). Optimization of instant edible films based on dietary fiber processed with dynamic high pressure microfluidization for barrier properties and water solubility. *LWT - Food Science and Technology, 60*(1), 603–608. https://doi.org/10.1016/j.lwt.2014.07.032

Wang, S., Li, C., Copeland, L., Niu, Q., & Wang, S. (2015). Starch retrogradation: A comprehensive review. *Comprehensive Reviews in Food Science and Food Safety, 14*(5), 568–585. https://doi.org/10.1111/1541-4337.12143

Zainuddin, S., Ahmad, I., Kargarzadeh, H., Abdullah, I., & Dufresne, A. (2013). Potential of using multiscale kenaf fibers as reinforcing filler in cassava starch-kenaf biocomposites. *Carbohydrate Polymers, 92*(2), 2299–2305. https://doi.org/10.1016/j.carbpol.2012.11.106